1 **300 years of Tropospheric Ozone changes using CMIP6 Scenarios with a**
2 **Parameterised Approach**

3 Steven T. Turnock[1], Oliver Wild[2], Alistair Sellar[1], Fiona M. O'Connor[1]

4 [1] Met Office Hadley Centre, Exeter, UK

5 [2] Lancaster Environment Centre, Lancaster University, Lancaster, UK

6 Correspondence: Steven Turnock (steven.turnock@metoffice.gov.uk)

7

8 **Abstract**

9 Tropospheric Ozone (O_3) is both an air pollutant and a greenhouse gas. Predicting changes
10 to O_3 is therefore important for both air quality and near-term climate forcing. It is
11 computationally expensive to predict changes in tropospheric O_3 from every possible future
12 scenario in composition climate models like those used in the 6th Coupled Model
13 Intercomparison Project (CMIP6). Here we apply the different emission pathways used in
14 CMIP6 with a model based on source-receptor relationships for tropospheric O_3 to predict
15 historical and future changes in O_3 and its radiative forcing over a 300 year period (1750 to
16 2050). Changes in regional precursor emissions (nitrogen oxides, carbon monoxide and
17 volatile organic compounds) and global methane abundance are used to quantify the impact
18 on tropospheric O_3 globally and across 16 regions, neglecting any impact from changes in
19 climate. We predict large increases in global surface O_3 (+8 ppbv) and O_3 radiative forcing
20 (+0.3 W m^{-2}) over the industrial period. Nine different Shared Socio-economic Pathways are
21 used to assess future changes in O_3. Scenarios involving weak air pollutant controls and
22 climate mitigation are inadequate in limiting the future degradation of surface O_3 air quality
23 and enhancement of near-term climate warming over all regions. Middle-of-the-road and
24 strong mitigation scenarios reduce both surface O_3 concentrations and O_3 radiative forcing by
25 up to 5 ppbv and 0.17 W m^{-2} globally, providing benefits to future air quality and near-term
26 climate forcing. Sensitivity experiments show that targeting mitigation measures towards
27 reducing global methane abundances could yield additional benefits for both surface O_3 air
28 quality and near-term climate forcing. The parameterisation provides a valuable tool for rapidly
29 assessing a large range of future emission pathways that involve differing degrees of air
30 pollutant and climate mitigation. The calculated range of possible responses in tropospheric
31 O_3 from these scenarios can be used to inform other modelling studies in CMIP6.

32 Keywords – Ozone, air quality, climate, radiative forcing, CMIP6

1.0 Introduction

Tropospheric Ozone (O_3) is an important trace gas in the atmosphere, and is both an air pollutant and a climate forcing agent. At the Earth's surface elevated concentrations of O_3 are harmful to human health (Jerrett et al., 2009; Malley et al., 2017; Turner et al., 2016) and can affect ecosystems (Fowler et al., 2009). O_3 in the troposphere acts as a greenhouse gas by interacting with outgoing longwave radiation, resulting in a net warming impact on climate of +0.4 (0.2 to 0.6) W m^{-2} over the industrial period (Myhre et al., 2013; Stevenson et al., 2013). The relatively short lifetime of O_3 in the troposphere (~3 weeks, Young et al., 2013) means that it is classified as a Near Term Climate Forcer (NTCF), having an important influence on climate over shorter timescales. Understanding how tropospheric O_3 changes is important for both future air quality and climate.

Tropospheric O_3 is a secondary pollutant that can be formed from both local and remote precursor emissions (Fiore et al., 2009). It is therefore influenced by both national and international emission control measures. Changes in global methane (CH_4) abundance and climate change also affect O_3 formation. These global changes are influenced by changes in future emission policies, adding additional uncertainty to the O_3 response (Fiore et al., 2012; Jacob and Winner, 2009; von Schneidemesser et al., 2015). It is therefore vital to consider the impact on tropospheric O_3 from a range of different future scenarios to ascertain which have beneficial effects over key regions.

A multi-model assessment of historical and future changes in tropospheric O_3 was made in the Atmospheric Chemistry and Climate Model Intercomparison Project (ACCMIP), using future changes in climate and O_3 precursor emissions from the Representative Concentration Pathways (RCPs) (Lamarque et al., 2013). The models participating in ACCMIP predicted changes in global annual mean surface O_3 concentrations between 2000 and 2030 of ±1.5 ppbv using the different RCPs (Young et al., 2013). More recent single model estimates by O'Connor et al., (2014) and Kim et al., (2015) predict a surface O_3 response across the different RCPS of between -4.0 to +2.0 ppbv by 2050 (relative to 2000). Global annual mean tropospheric O_3 burden was predicted to change by between -18% and +20% from 2000 to 2100 in the different RCPs (Cionni et al., 2011; Kawase et al., 2011; O'Connor et al., 2014; Young et al., 2013). For the ACCMIP models, Stevenson et al., (2013) calculated that tropospheric O_3 radiative forcing (relative to 2000) varies between -0.05 and +0.08 W m^{-2} in 2030 and between -0.19 and +0.22 W m^{-2} in 2100 across the range of the RCPs. For RCP8.5, Iglesias-Suarez et al., (2018) predicted a whole atmosphere O_3 radiative forcing of +0.43 ± 0.11 W m^{-2} in 2100 (relative to 2000), with +0.3 ± 0.05 W m^{-2} due to tropospheric O_3 and +0.13 ± 0.04 W m^{-2} from stratospheric O_3. Future tropospheric O_3 may therefore either increase or decrease depending on the mitigation measures assumed in the scenario. In addition, the spread of the model responses in ACCMIP can be as much as 50% of the reported multi-model mean values, highlighting the large uncertainty in the future prediction of tropospheric O_3 across different models.

ACCMIP formed part of the 5th Coupled Model Intercomparison Project (CMIP5) and used air pollutant precursor emissions that spanned a relatively narrow range of future trajectories in the RCPs (Rao et al., 2017). In preparation for the 6th CMIP (CMIP6) a new set of historical and future pathways have been created. Five different socio-economic pathways (SSPs) have been developed with centennial trends based on different combinations of social, economic and environmental developments (O'Neill et al., 2014). Different levels of emission mitigation

78 are included within a specific SSP, to meet a particular climate target and a defined amount
79 of air pollution control (Rao et al., 2017; Riahi et al., 2017). The SSPs allow for a wider range
80 of future trajectories in air pollutant precursors to be explored than was possible in CMIP5 with
81 the RCPs.

82 Here we utilise the historical and future scenarios used in CMIP6 with the parameterised
83 approach of Turnock et al., (2018) to quantify the response of tropospheric O_3 to changes in
84 regional precursor emissions and global CH_4 abundances. The parameterisation uses source-
85 receptor relationships derived from the response of models to emission precursor perturbation
86 experiments, conducted as part of Phase 2 of the Hemispheric Transport of Air Pollutants
87 (HTAP) project (Turnock et al., 2018). Whilst it is not intended to replace full atmospheric
88 chemistry simulations, the parameterisation allows rapid assessment and provides a first look
89 at the impact of all future CMIP6 scenarios on surface O_3 air quality and near-term O_3 radiative
90 forcing. It calculates the response of tropospheric O_3 across the industrial period and to all
91 available future SSPs, permitting simple identification of the most interesting SSPs to
92 investigate in more detail using the current generation of chemistry, climate and Earth system
93 models.

94 In this paper we briefly describe the historical emissions and those in the SSPs that are used
95 with the parameterisation to predict changes in tropospheric O_3 and its radiative forcing. We
96 quantify changes in surface O_3, tropospheric O_3 burden and O_3 radiative forcing over the
97 historical period (1750 to 2014) and provide the first results from future scenarios used in
98 CMIP6 (2015 to 2050, when the impact of climate change is relatively small). The O_3 response
99 is solely due to changes in anthropogenic emissions of O_3 precursors and CH_4 abundance,
100 neglecting any impact from climate change. Here, we extend the analysis with a limited
101 number of CMIP6 scenarios by attributing changes in O_3 to anthropogenic emission source
102 sectors and by using idealised experiments to explore the impact on O_3 of mitigation measures
103 solely targeting CH_4. Finally, we summarise how different policy measures in the SSPs impact
104 future surface O_3 air quality and O_3 climate forcing.

105 **2.0 Methods**

106 *2.1 Ozone Parameterisation*

107 The approach used in this study is a parameterisation of O_3 changes developed previously by
108 Wild et al., (2012) and Turnock et al., (2018). The parameterisation uses the source-receptor
109 relationships from models participating in the HTAP project, derived from perturbation
110 experiments of regional precursor emissions and global CH_4 abundances. The input to the
111 parameterisation is the individual model O_3 response to changes in global CH_4 abundance
112 and to 20% reductions of nitrogen oxide (NOx), carbon monoxide (CO) and non-methane
113 volatile organic compound (NMVOC) emissions within each source region (14 source regions
114 in total over the globe, see Figure S1). The parameterisation accounts for the effect of
115 emission and CH_4 changes on O_3 but neglects any influence from changes in climate, as the
116 HTAP simulations were performed for a single meteorological year corresponding to 2010.

117 For a particular emission scenario, the fractional precursor emission (NOx, CO, NMVOCs)
118 and CH_4 abundance change (*r*) is calculated relative to the original 20% emission (*E*)
119 perturbation (Eq. 1). This linear emission scaling factor is applied to the O_3 response for
120 changes in CO and NMVOCs (Eq. 2), but a non-linear scaling factor (Eq. 3) is used for
121 changes in NOx and CH_4 and (Eq. 4) for conditions where O_3 titration occurs (an O_3 increase

122   for a decrease in NOx). For each source region the multi-model monthly O_3 response (Eq. 5)
123   from the 20% emission perturbation experiments (ΔO_3 for emissions of NOx, CO and
124   NMVOCs and ΔO_{3m} for CH_4) are then scaled by the relevant emission scaling factor (f). The
125   total monthly mean O_3 response (ΔO_3) over each receptor region (k) is the sum of the
126   individual O_3 responses from each model to global CH_4 changes and the different emission
127   precursors (i) across all source regions (j).

128   $r_{ij} = \frac{\Delta E_{ij}}{-0.2 \times E_{ij}} \ or \ \frac{\Delta [CH_4]}{-0.2 \times [CH_4]}$ (1)

129   $f_{ij} = r_{ij}$ $Linear \ Scaling \ of \ O_3 response$ (2)

130   $f_{ij} = 0.95 r_{ij} + 0.05 r_{ij}^2$ $Scaling \ accounting \ for \ reduced \ O_3 \ increases \ from \ NO_X \ and \ CH_4$ (3)

131   $f_{ij} = 1.05 r_{ij} - 0.05 r_{ij}^2$ $Scaling \ for \ titration \ regimes \ where \ decreasing \ NO_X \ increases$ (4)

132   $\Delta O_3(k) = \sum_{i=1}^{3} \sum_{j=1}^{5} f_{ij} \Delta O_{3e}(i,j,k) + f_m \Delta O_{3m}(k)$ (5)

133   The parameterisation provides the global and regional O_3 response at the surface and
134   throughout the troposphere. The O_3 radiative forcing is then derived from the change in
135   tropospheric O_3 burden using the multi-model ensemble mean relationship from ACCMIP
136   (Stevenson et al., 2013). In this way the parameterisation can be used to rapidly assess the
137   impact of changes in precursor emissions and CH_4 abundance on surface O_3 air quality and
138   near term climate forcing due to O_3. In addition, a measure of uncertainty is generated by the
139   parameterisation based on the range of HTAP multi-model responses.

140   We have updated the parameterisation used in Turnock et al., (2018) to rectify some small
141   coding errors subsequently found in the calculation of tropospheric O_3 burden and O_3 radiative
142   forcing. Table S1 reproduces Table 10 of Turnock et al., (2018) but includes results from the
143   updated parameterisation used here. The surface O_3 response is unaffected by the updates,
144   but the tropospheric O_3 burden and O_3 radiative forcing are reduced compared to that in
145   Turnock et al., (2018), although still within or at the lower end of the range of the ACCMIP
146   multi-model response.

147   The parameterisation has previously been shown to reproduce the O_3 response to different
148   emission perturbations from full model simulations (Turnock et al., 2018; Wild et al., 2012).
149   Here we use the parameterisation to quantify the O_3 response to CMIP6 historical emissions
150   and to the full range of future SSPs, which include differing climate mitigation targets and
151   various levels of air pollutant control. Using a combination of historical and future emissions
152   we calculate 300 years of changes to tropospheric O_3. Further experiments are conducted
153   with the parameterisation to attribute the change in tropospheric O_3 from different emission
154   source sectors and the impact from mitigation scenarios solely targeting reductions in CH_4.

155   *2.2 CMIP6 Emissions*

156   A new set of historical anthropogenic emissions has been developed with the Community
157   Emissions Data System (CEDS) (Hoesly et al., 2018). CEDS uses updated emissions factors
158   to provide monthly emissions of the major aerosol and trace gas species over the period 1750
159   to 2014 for use in CMIP6, and includes the interannual variation in biomass burning.

160   The SSPs used in CMIP6 represent an update from CMIP5 as they combine pathways of
161   different greenhouse gas concentrations (RCPs) with new scenarios of socio-economic

162 development that encompass a range of challenges to mitigation and adaption (O'Neill et al.,
163 2014; van Vuuren et al., 2014). Five different baseline SSPs (1-5) are used to represent
164 different combinations of future social, environmental and economic development over the 21st
165 Century (O'Neill et al., 2014; Riahi et al., 2017). The SSPs vary from those with lower resource
166 and energy use (sustainability - SSP1) to those focussing on energy intensification and fossil
167 fuel use (SSP5). Mapped onto each SSP is an assumption about the degree of air pollution
168 control (strong, medium or weak), representing the different speeds and technological
169 pathways to meet targets. Rising income levels and stricter air pollution controls are assumed
170 to occur together, as control technology costs are lowered and a greater emphasis is placed
171 on improving human health (Rao et al., 2017). This allows the SSPs to cover a wider range of
172 future air pollutant emission trajectories in a greater number of scenarios than was possible in
173 CMIP5, and supports the need for a rapid assessment tool to evaluate all scenarios.

174 The baseline SSPs are unable to reach lower radiative forcing targets and result in a climate
175 radiative forcing of 5.0 – 8.7 W m^{-2} by 2100 (Riahi et al., 2017). Different greenhouse gas
176 mitigation strategies are introduced on top of each baseline SSP to achieve a defined climate
177 radiative forcing target in 2100. A wide range of measures are used to achieve emission
178 reductions and reflect the specific storyline of the SSP, e.g., carbon capture and storage,
179 increased use of renewables, reduced agriculture emissions and afforestation. A summary of
180 each scenario used in this study is shown in Table 1, with further details on each pathway
181 presented in O'Neill et al., (2014), Rao et al., (2017), Riahi et al., (2017) and (Gidden et al.,
182 2019).

183 **Table 1** – Summary of all CMIP6 scenarios with gridded emissions that are used in this study

Scenario	SSP Narrative	Challenges for:		Climate Target (radiative forcing by 2100, W m^{-2})	Level of Air Pollution Controls
		Mitigation	Adaption		
SSP1 1.9	Sustainability	Low	Low	1.9	Strong
SSP1 2.6	Sustainability	Low	Low	2.6	Strong
SSP2 4.5	Middle of the Road	Medium	Medium	4.5	Medium
SSP3 7.0	Regional Rivalry	High	High	7.0	Weak
SSP3 7.0 lowNTCF	Regional Rivalry	High	High	6.3*	Strong
SSP4 3.4	Inequality	Low	High	3.4	Weak
SSP4 6.0	Inequality	Low	High	6.0	Weak
SSP5 3.4	Fossil-fuelled Development	High	Low	3.4	Strong
SSP5 8.5	Fossil-fuelled Development	High	Low	8.5	Strong

184 * Climate target is lowered due to reduced contribution of NTCFs to end of century warming (Gidden et al., 2019).

185 In this study we have used changes in CH$_4$ abundance and anthropogenic emissions of NOx,
186 CO and NMVOCs from the historical dataset and nine SSPs developed for CMIP6 (Table 1).
187 Similar climate forcing targets to those used in CMIP5 are included within SSP1 2.6, SSP2
188 4.5, SSP3 7.0 and SSP5 8.5 scenarios. Additional scenarios with differing levels of climate
189 mitigation (SSP1 1.9, SSP3 lowNTCF, SSP4 3.4, SSP4 6.0 and SSP5 3.4) are provided for
190 CMIP6. The radiative forcing targets range from a strong mitigation scenario of 1.9 W m^{-2},
191 which keeps temperatures well below 2°C by 2100 (in accordance with the Paris Agreement,
192 (United Nations, 2016)), to a weak mitigation scenario with a radiative forcing of 8.5 W m^{-2},
193 resulting in a temperature change of ~5°C by 2100 (Riahi et al., 2017). SSP3 7.0 lowNTCF is
194 provided for the Aerosol and Chemistry Model Intercomparison Project (AerChemMIP)
195 experiments (Collins et al., 2017) and represents a direct comparison to SSP3 7.0 but with
196 substantially reduced NTCFs. SSP4 scenarios are included to study pathways with low

197 mitigation challenges that have strong land use and aerosol-climate effects (Gidden et al.,
198 2019). SSP5 3.4 is a delayed mitigation scenario which follows the same pathway as SSP5
199 8.5 up until 2040 but then implements policy measures to reduce warming in the latter half of
200 the century.
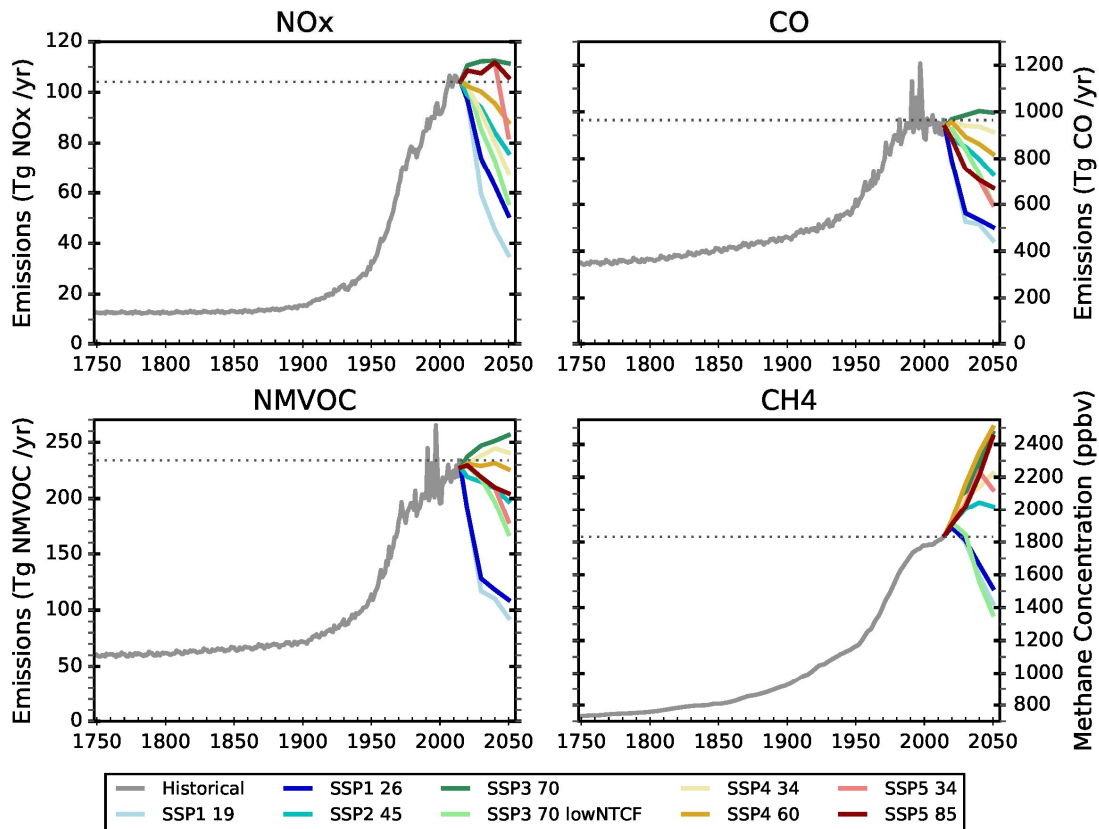
201

202 **Figure 1** – Global total annual emissions of NOx, CO and NMVOCs and the global CH4 abundance
203 from the CMIP6 historical and future scenarios dataset.

204 Figure 1 shows the global change in the emission of air pollutants (NOx, CO and NMVOCs)
205 and CH_4 abundance over the period 1750 to 2014 in the historical emissions and in the nine
206 different future SSPs from 2015 to 2050. Global emissions of air pollutants remain low up until
207 the early part of the 20th Century. In the second half of the 20th Century global emissions rapidly
208 increase in response to industrialisation, particularly over Europe, North America and Asia
209 (Table S2). On a global basis, SSP3 7.0 is the only scenario where global air pollutant
210 emissions are not declining (relative to 2015). Large reductions in all air pollutant emissions
211 are seen across all regions in SSP3 7.0 lowNTCF and the SSP1s (Table 1 and Table S3-S4)
212 due to large reductions in the energy, industrial, residential and transport sectors (Figures S2-
213 S4, Tables S5-S7). In SSP3 7.0 and SSP5 8.5 air pollution emissions tend to increase in most
214 regions, apart from Europe and North America. Emissions decrease across most regions in
215 the SSP2 and SSP4 scenarios, apart from in South Asia where emissions increase for almost
216 all scenarios, mainly from the energy, industrial and transport sectors (Figure S5).

217 CH_4 abundances show a continuous increasing trend over the historical period from 731 ppbv
218 in 1750 to 1831 ppbv in 2014, with the most rapid changes occurring since the 1950s. Over
219 the period 2015 to 2050 most of the future scenarios show an increase in global CH_4

abundance of between 10% and 36%, apart from the three scenarios with the strongest climate and air pollutant mitigation (SSP1 1.9, SSP1 2.6 and SSP3 7.0 lowNTCF), where CH_4 abundance reduces by 18% to 26% (Table 2).

Table 2 – Percentage change in global methane abundance and in global and regional total (anthropogenic, shipping and biomass burning sectors) annual NOx emissions in 2050, relative to 2015, over each source region for the different CMIP6 emission scenarios. Positive changes are shown in bold. Regions are as defined in Figure S1.

|	Annual Total Emissions Change in 2050 (%) from 2015								
Region	SSP1 1.9	SSP1 2.6	SSP2 4.5	SSP3 7.0	SSP3 7.0 NTCF	SSP4 3.4	SSP4 6.0	SSP5 3.4	SSP5 8.5
Global CH_4	-22	-18	**+10**	**+34**	-26	**+21**	**+36**	**+15**	**+33**
Global NOx	-66	-51	-27	**+7**	-46	-35	-15	-21	**+2**
Central America	-58	-42	-20	**+27**	-51	-41	-25	0	**+32**
Central Asia	-32	-6	**+11**	**+27**	-37	-26	-11	-13	**+4**
East Asia	-79	-68	-53	**+17**	-44	-61	-27	-29	-12
Europe	-79	-74	-50	-38	-58	-64	-43	-34	-14
Middle East	-77	-55	-22	**+46**	-63	-42	-25	-39	-12
North Africa	-45	-4	**+10**	**+54**	-46	-1	**+18**	**+10**	**+51**
North America	-82	-74	-59	-37	-60	-61	-45	-49	-29
North Pole	-92	-86	-36	-43	-84	-56	-48	-46	-32
Ocean	-88	-78	-29	-27	-79	-47	-34	-35	-14
Pacific Aus NZ	-52	-46	-37	-13	-42	-32	-18	-22	-14
Rus Bel Ukr	-56	-50	-17	-14	-60	-59	-37	-42	-26
South America	-59	-46	-23	**+13**	-38	-39	-18	-9	**+12**
South Asia	-59	-25	**+29**	**+72**	**+3**	**+11**	**+50**	**+12**	**+52**
South East Asia	-49	-26	-24	**+33**	-31	**+46**	**+18**	-22	**+6**
Southern Africa	-10	**+3**	-14	-8	-33	-9	-2	**+9**	**+25**

3.0 Results

3.1 Historical Changes

The parameterisation reveals that global annual mean surface O_3, tropospheric O_3 burden and O_3 radiative forcing (± 1 standard deviation) increased by 7.6 ± 0.7 ppbv, 73 ± 8.9 Tg and 0.29 ± 0.03 W m^{-2} over the period 1850 to 2014 (Table 3 and Figure 2). The change in these variables over the period 1850 to 2000 simulated by the ACCMIP models is 10 ± 1.6 ppbv, 98 ± 17 Tg and 0.36 ± 0.06 W m^{-2} respectively (Stevenson et al., 2013; Young et al., 2013), slightly larger than the changes from the parameterisation. The large standard deviations show that there is a substantial diversity in model responses in the ACCMIP results. UKESM1, an Earth system model conducting experiments for CMIP6 (Sellar et al., 2019, in prep.), and a successor to the HadGEM2 model used for building the parameterisation, gives global changes of 7.3 ± 0.4 ppbv in surface O_3 and 66.7 ± 5.1 Tg in O_3 burden, very similar to the parameterisation (Figure 2).

The parameterisation does not account for the impacts on tropospheric O_3 from changes in stratosphere-to-troposphere exchange, chemical regime (O_3 production/titration) or climate,

243 which could explain the discrepancy with the ACCMIP models. A discrepancy could also occur
244 from the use of the different emission datasets in ACCMIP and CMIP6, but a comparison with
245 the parameterisation itself found this contribution to be very small. Within ACCMIP some
246 models calculated the impact of climate change over the historical period by conducting
247 experiments with a varying climate and emissions fixed at 1850 values. These models
248 calculated that climate change has a relatively small impact on tropospheric O_3 over the
249 industrial period, reducing the change in surface O_3, O_3 burden and O_3 radiative forcing by 2.7
250 ppbv, 22 Tg and 0.024 W m^{-2} respectively (Stevenson et al., 2013; Young et al., 2013). Most
251 of this reduction is anticipated to occur from enhanced O_3 destruction due to increases in water
252 vapour from rising temperatures (Doherty et al., 2013). If the reduction in tropospheric O_3 due
253 to the effects of climate change is removed from the ACCMIP estimate of change in O_3 over
254 the industrial period, then there is better agreement with the estimate of historical change from
255 the parameterisation.

256 There is no agreed observed change in tropospheric O_3 over the industrial period due to the
257 absence of reliable measurements (Young et al., 2018). Chemistry-climate models are only
258 able to reproduce half of the observed trend in O_3 over the second half of the 20th Century,
259 when reliable measurements are available and most of the change in O_3 occurred (Gaudel et
260 al., 2018; Young et al., 2018). Tropospheric O_3 changes from the parameterisation over the
261 industrial period are consistent with those from ACCMIP models and UKESM1 but all tend to
262 underestimate the measured change.

263 Figure 2 shows that surface O_3, tropospheric O_3 burden and O_3 radiative forcing rapidly
264 increase through the 20th Century, coinciding with the largest changes in emissions and CH_4
265 (Figure 1). Larger regional increases in annual mean surface O_3 of >10 ppbv occur over
266 Europe, North America, Asia and the Middle East (Table 3 and Figure S6). The changes in
267 annual mean surface O_3 since 1750 show the impact of industrialisation and increasing
268 emissions over the 20th century across most regions. However, they also show the more recent
269 decline in surface O_3 concentrations across Europe and North America (<2 ppbv) over the last
270 30 years due to the reduction in precursor emissions from the implementation of air pollution
271 controls. Historical changes in tropospheric O_3 over the industrial period provide a context in
272 which to frame the predicted changes from different future scenarios.

273
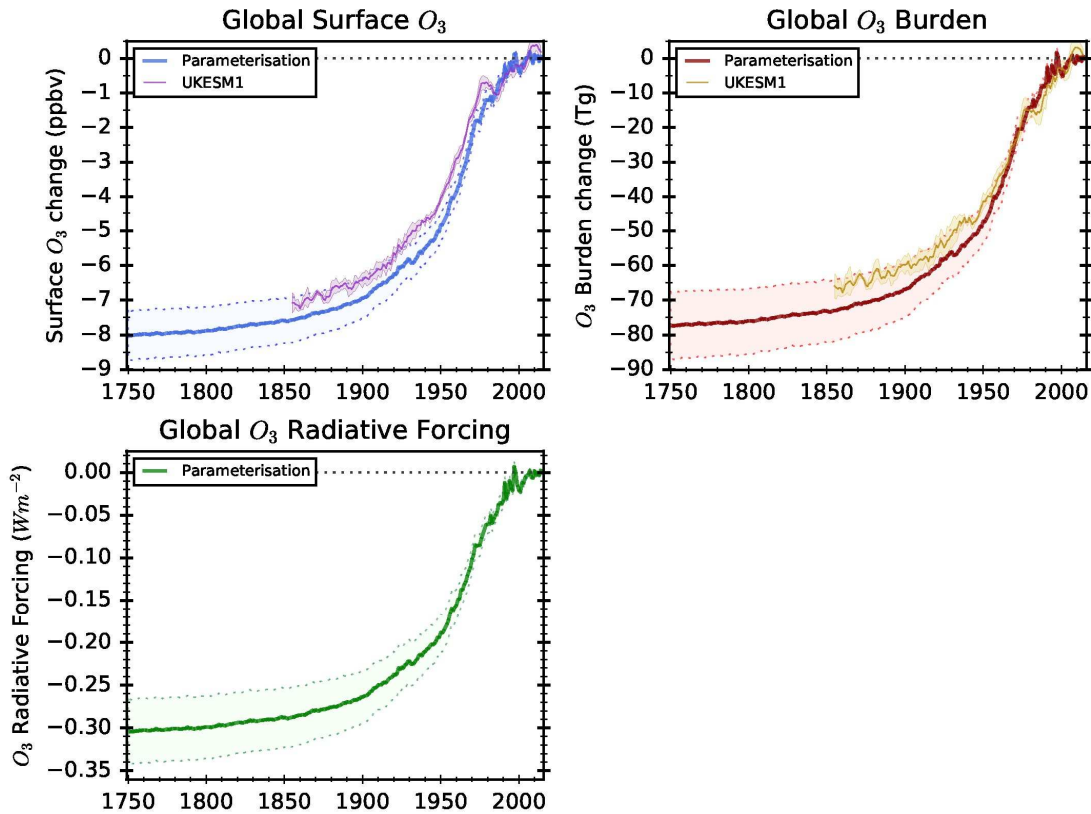
Figure 2 – Change in the global annual mean surface O_3 concentrations, total O_3 burden and O_3 radiative forcing over the historical period, relative to 2014, from the parameterisation using historical emissions provided for CMIP6. A 5-year running mean of the change in global surface O_3 concentrations and total O_3 burden, relative to 2014, is also shown from UKESM1. Shaded areas show the spread in the response from the multi-model parameterisation and ensemble members of UKESM1 (±1 standard deviation).

Table 3 – Regional and global change in annual mean surface O_3 concentrations over the historical period, relative to 2014.

|	Δ Surface O_3 (ppbv)					
Region	**1750**	**1850**	**1900**	**1950**	**1980**	**2000**
Global	-7.9	-7.6	-6.9	-4.8	-1.2	-0.4
Central America	-9.1	-8.7	-8.2	-5.3	-1.0	+0.5
Central Asia	-10.6	-9.9	-8.8	-5.8	+0.9	+0.4
East Asia	-12.9	-12.4	-11.5	-8.7	-2.5	-1.2
Europe	-10.5	-9.6	-8.3	-5.0	+2.0	+1.0
Middle East	-17.6	-16.8	-15.7	-11.9	-3.4	-1.0
North Africa	-12.2	-11.6	-10.4	-6.9	-0.1	+0.4
North America	-10.8	-10.1	-9.1	-4.5	+1.0	+0.7
North Pole	-7.8	-7.3	-6.6	-4.2	+0.2	+0.2
Ocean	-7.8	-7.4	-6.9	-4.8	-1.4	-0.4
Pacific Aus NZ	-4.7	-4.5	-4.0	-3.0	-1.2	-0.3
Rus Bel Ukr	-7.9	-7.4	-6.5	-4.0	+0.4	+0.2
South America	-4.6	-4.4	-4.1	-3.2	-1.5	-0.5
South Asia	-17.7	-17.1	-16.3	-13.6	-6.9	-3.8
South East Asia	-9.7	-9.5	-9.1	-7.7	-4.8	-2.9
South Pole	-3.5	-3.3	-3.0	-2.2	-0.9	-0.3
Southern Africa	-5.1	-4.8	-4.4	-3.1	-1.1	-0.3

3.2 Future Scenarios

The nine CMIP6 SSPs (Table 1) are used with the O_3 parameterisation to predict the impact on tropospheric O_3 over the near-term future (2015 to 2050), when effects of climate are likely to be small (Doherty et al., 2017; Fiore et al., 2015). Figure 3 shows that there are a variety of responses in global annual mean surface O_3, O_3 burden and O_3 radiative forcing to the different SSPs. The predictions from the parameterisation are compared to the global mean changes simulated by UKESM1 for four representative SSPs.

The three strong mitigation pathways (SSP1 1.9, SSP1 2.6 and SSP3 7.0 lowNTCF) all show (relative to 2015) large reductions of >3.5 ppbv in surface O_3, >30 Tg in O_3 burden and an O_3 radiative forcing of <-0.1 W m^{-2} in 2050, due to the large reductions in precursor emissions and CH_4. Figure 3 shows that the global changes in surface O_3 and O_3 burden in 2050 from the parameterisation are consistent with those simulated using UKESM1. Using the simplified expression of Etminan et al., (2016) a direct CH_4 radiative forcing of <-0.15 W m^{-2} is calculated for the strong mitigation scenarios, providing an additional direct benefit to climate on top of the reduction in O_3 forcing. However, the benefits to surface air quality and near-term climate forcing in the most ambitious mitigation scenarios are still less than half of the changes that occurred over the industrial period.

The middle of the road scenario (SSP2 4.5) is predicted to have slightly reduced global surface O_3 concentration, O_3 burden and O_3 radiative forcing in 2050 compared to 2015. In this scenario decreases in precursor emissions are offset by increases in global CH_4 abundance of 10%. The global changes predicted by the parameterisation are again in agreement with those from UKESM1, which shows a slight reduction in surface O_3 and O_3 burden.

All the weak mitigation scenarios (SSP 7.0, SSP5 8.5 and SSP4 6.0) are predicted to increase global annual mean surface O_3 by up to 1.5 ppbv, O_3 burden by up to 18 Tg and O_3 radiative forcing by up to +0.07 W m^{-2} in 2050. The predicted changes in surface O_3 and O_3 burden for SSP5 8.5 are consistent with those from UKESM1. For SSP3 7.0 the predicted increases in O_3 are larger than those in UKESM1, particularly over South Asia (Figure S7). These regions experience large increases in NOx emissions of up to 70% in SSP3 7.0, resulting in changes in chemical regime from O_3 production to O_3 titration. This change in chemical regime cannot be captured with the parameterisation and it therefore overestimates the O_3 response in these regions, as previously shown in Turnock et al., (2018). A direct CH_4 radiative forcing of up to +0.27 W m^{-2} is calculated using the simplified expression of Etminan et al., (2016) for the weak SSP mitigation scenarios. This is in addition to the positive forcing from O_3, which will both have a detrimental effect on climate. The large global increase in CH_4 abundance in these scenarios, of up to 36%, offsets any benefits to O_3 from reducing precursor emissions, highlighting the importance of controlling future CH_4 emissions for reducing tropospheric O_3.
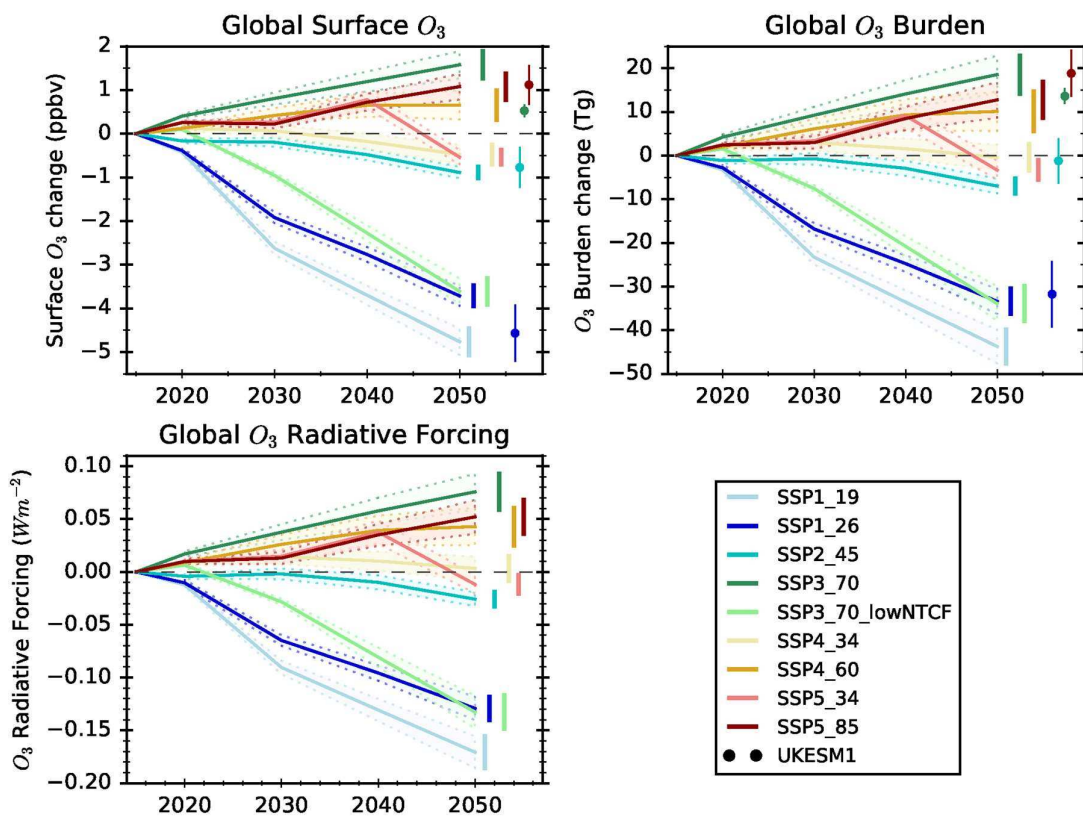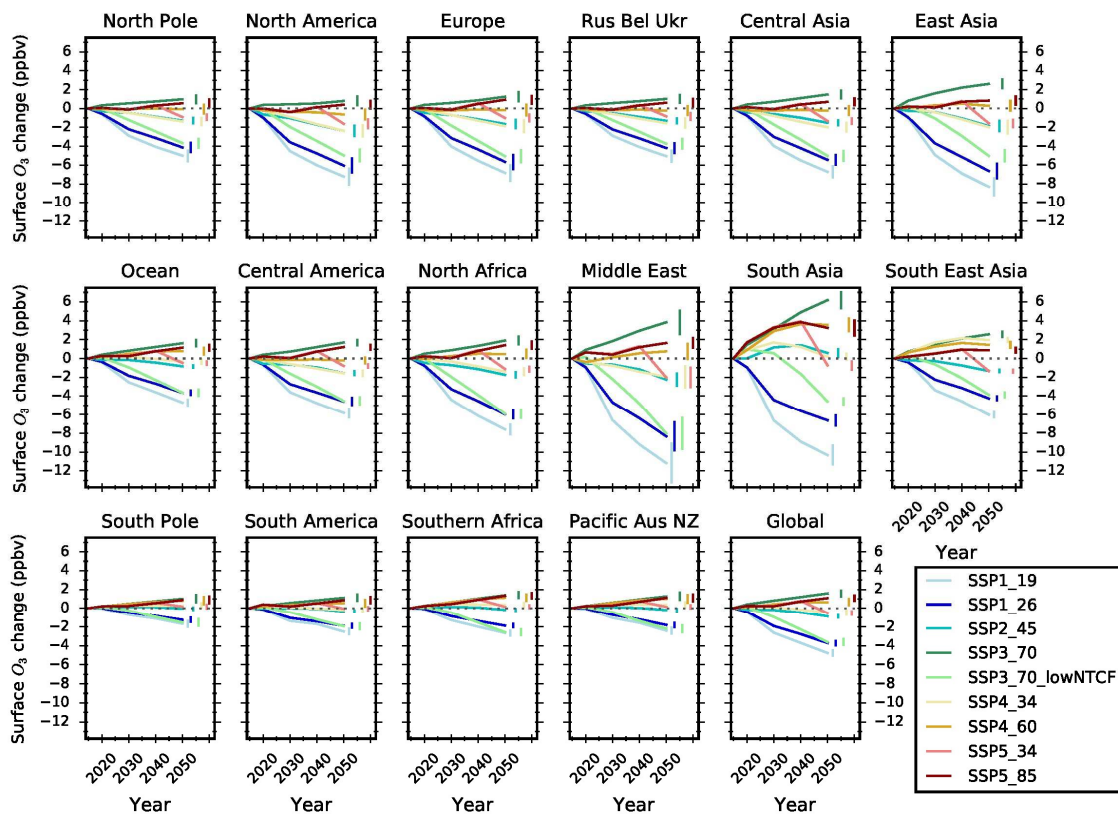
Figure 3 – Changes in global annual mean surface O_3 concentrations, total O_3 burden and O_3 radiative forcing, relative to 2015, from the parameterisation for different future CMIP6 pathways. Shaded area shows the spread in multi-model response (±1 standard deviation). The spread in multi-model response in 2050 is represented by the vertical line at the end of each plot. The change in surface O_3 and O_3 burden (±1 standard deviation) simulated by UKESM1 in 2050 is represented by the circles at the far end of the plot.

Figure 4 and Table S8 show that there is a large range in annual regional mean surface O_3 responses for the nine SSPs. The largest range occurs over the Middle East and South Asia where a reduction of >10 ppbv (relative to 2015) is predicted for the strong mitigation scenario (SSP1 1.9) and an increase of >3 ppbv is predicted for the weak mitigation scenario (SSP3 7.0). However, the range in O_3 responses over these particular regions may be overestimated with the parameterisation, as noted above. Across Europe, North America and East Asia, the range of response in surface O_3 is smaller but reductions of >6 ppbv occur in the strong mitigation scenarios where precursor emissions and CH_4 abundances are heavily reduced. However, even the most ambitious mitigation scenario results in regional annual mean surface O_3 concentrations over Europe and North America that are 30% greater than estimated for the pre-industrial period (Figure S6).

For the weak mitigation scenario of SSP3 7.0 surface O_3 increases by 2.6 ppbv for East Asia and by ~1 ppbv for Europe and North America. Increases in surface O_3 occur in both SSP3 7.0 and SSP5 8.5 due to the >30% increase in global CH_4 abundances, despite reductions in NOx emissions. This again highlights the importance of implementing both local and hemispheric emission control measures, particularly for CH_4, to control future regional changes in surface O_3.

342

Figure 4 – Changes in global and regional annual mean surface O$_3$ concentrations, relative to 2015, for different future CMIP6 pathways. The spread in multi-model response in 2050 is represented by the vertical line at the end of each plot (±1 standard deviation).

A source attribution is presented for selected SSPs for East Asia (Figure 5) and South Asia (Figure 6) to show the influence of local and remote emission sources on surface O$_3$. Across East Asia the contribution of locally formed O$_3$ to the total surface O$_3$ response in 2050 decreases by up to 2.8 ppbv across most scenarios due to the reduction of local emissions. SSP3 7.0 is an exception to this, as local emissions increase and consequently the O$_3$ response increases by 0.5 ppbv in 2050. The influence from regions external to East Asia is shown to be important in achieving reductions in regional surface O$_3$, particularly for the stronger mitigation scenarios where reductions of more than 1 ppbv can be achieved. In most scenarios, apart from SSP1 1.9, global CH$_4$ abundances rise and contribute to an increase in surface O$_3$ of up to 2 ppbv.

Over South Asia, local emission sources are more important in influencing the total O$_3$ response and counteract changes from external source regions. Large reductions in surface O$_3$ concentrations are achieved in the strong mitigation scenario from local (-4.8 ppbv), remote (-4.1 ppbv) and CH$_4$ (-1.5 ppbv) sources. However, in the medium and weak mitigation scenarios surface O$_3$ increases from local emissions (up to +4.1 ppbv) and global CH$_4$ abundance (up to +1.9 ppbv). This increase outweighs any reductions in O$_3$ obtained from emission sources remote to South Asia (up to -1.6 ppbv).

This analysis of source contributions highlights that local emission reductions are not always enough to reduce regional surface O$_3$ concentrations in the future. Emission controls on a

hemispheric scale are also required, particularly for CH_4, to reduce transboundary sources of

O_3 and keep the regional surface O_3 below present-day concentrations.

367
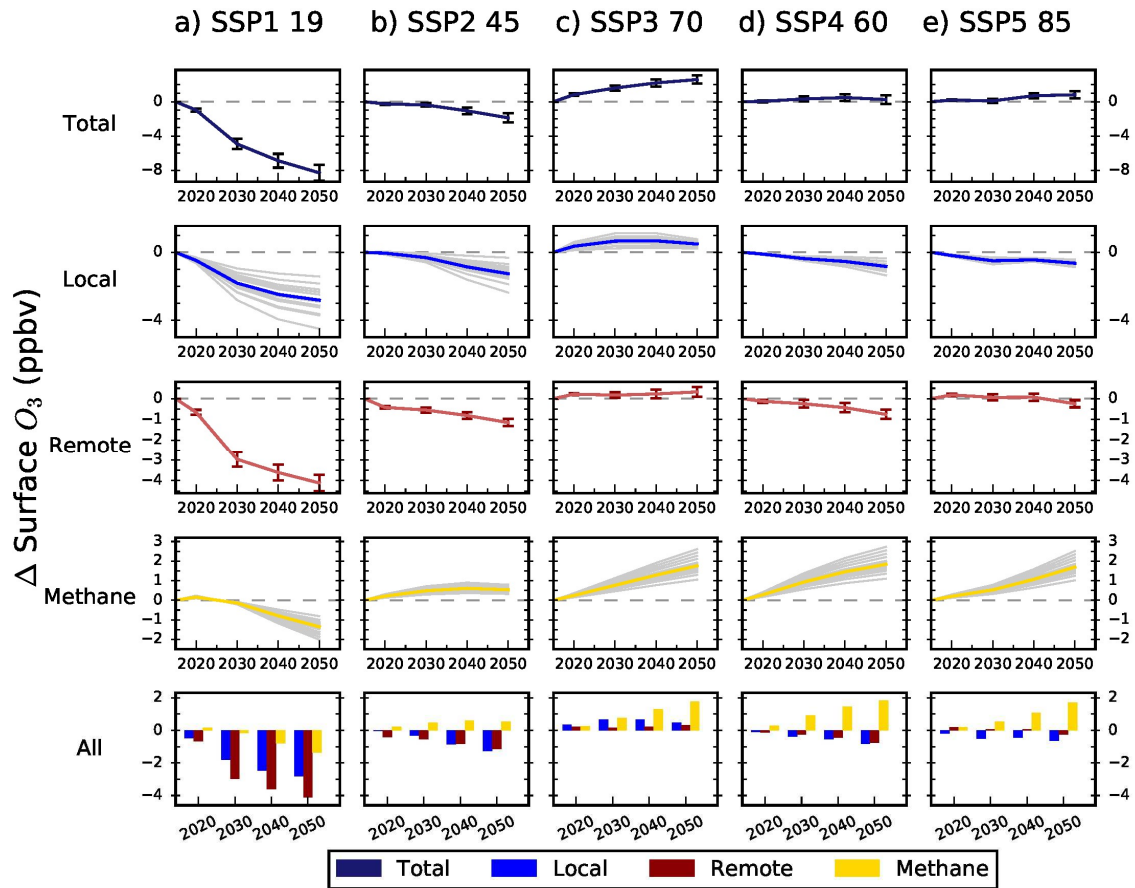
Figure 5 - Total annual mean changes in regional surface O_3 concentrations over East Asia and the contribution of local (blue), remote (red) and methane (gold) sources between 2015 and 2050 from the parameterisation for the CMIP6 emissions under the a) SSP1 1.9, b) SSP2 4.5, c) SSP3 7.0, d) SSP4 6.0 and e) SSP5 8.5 scenarios. Grey lines on the local and methane panels represent individual model estimates of O_3 changes, showing the spread in model responses; solid lines show the multi-model mean. Error bars represent one standard deviation over the entire multi-model range. The bottom panels show the O_3 response from individual sources plotted together.
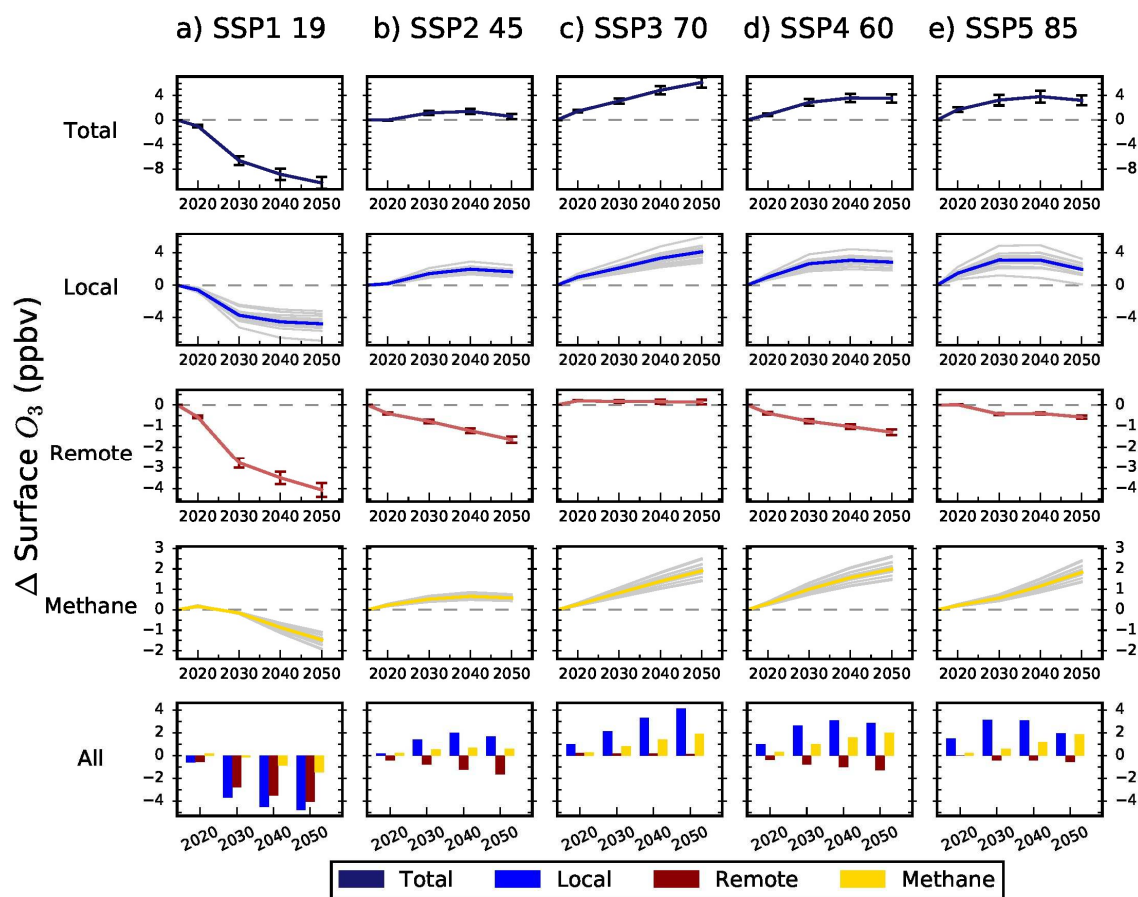
Figure 6 - Total annual mean changes in regional surface O_3 concentrations over South Asia and the contribution of local (blue), remote (red) and methane (gold) sources between 2015 and 2050 from the parameterisation for the CMIP6 emissions under the a) SSP1 1.9, b) SSP2 4.5, c) SSP3 7.0, d) SSP4 6.0 and e) SSP5 8.5 scenarios. Grey lines on the local and methane panels represent individual model estimates of O_3 changes, showing the spread in model responses; solid lines show the multi-model mean. Error bars represent one standard deviation over the entire multi-model range. The bottom panels shows the O_3 response from individual sources plotted together.

3.3 Emission Source Sectors

We have used the fractional emission change from different emission source sectors, relative to the total (Figures S2-S4, Tables S5-S7), to understand their contribution to the overall response in annual mean surface O_3 and O_3 radiative forcing in four SSPs (SSP1 1.9, SSP2 4.5, SSP3 7.0, SSP5 8.5). The sum of the O_3 response from the individual source sectors closely matches (within 7%) the combined O_3 response in each scenario (Figure 7).
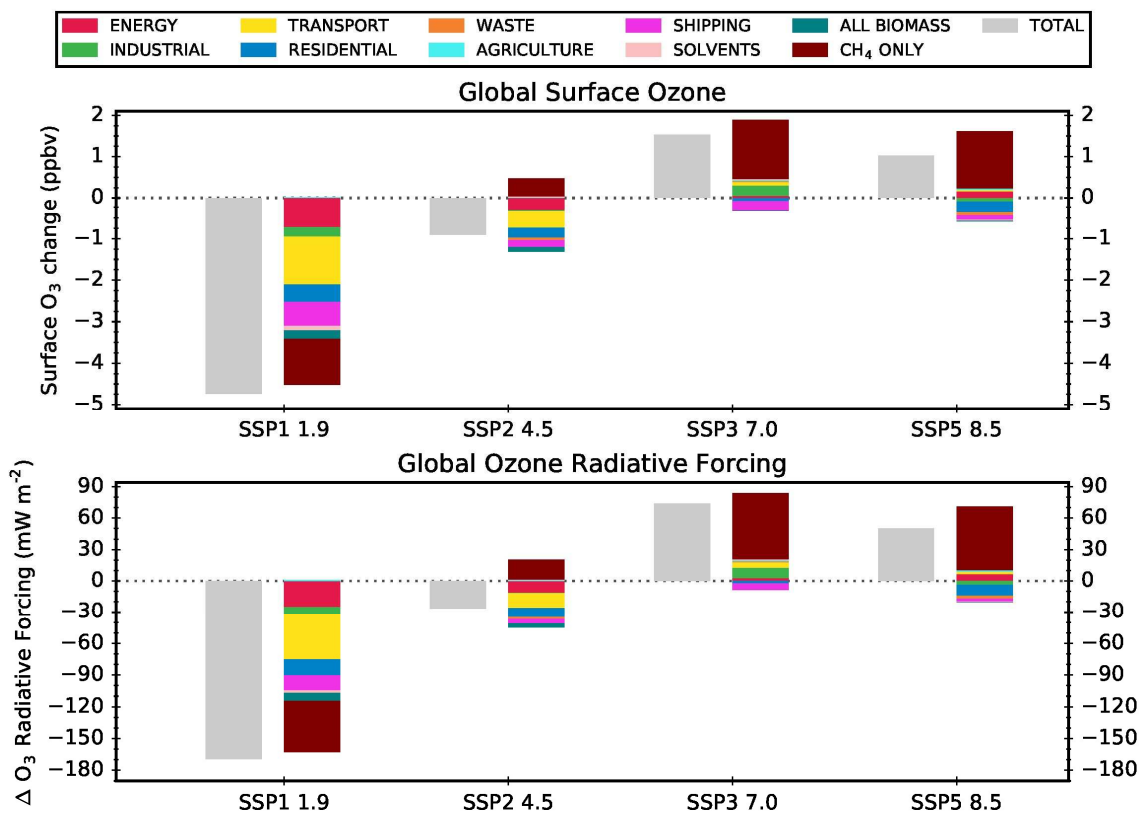
Figure 7 – Changes in global annual mean surface O_3 concentrations (ppbv) and O_3 radiative forcing (mW m^{-2}) due to individual emission sectors and the total overall response between 2015 and 2050 using four different CMIP6 future scenarios.

Figure 8 shows the surface O_3 response from each source sector in 2050 across four regions. Both Figures 7 and 8 show that the dominant driver of changes in surface O_3 both globally and regionally is changes in CH_4 abundance. An analysis of individual source sectors contributing to CH_4 emissions shows that the largest changes occur in the energy, waste and agricultural sectors (Figure S8). Globally, other emission source sectors make smaller contributions to surface O_3. The energy, industrial, transport and residential source sectors are more important regionally. Strong emission controls in these sectors, particularly on transport, could reduce surface O_3 by up to 2 ppbv over Europe and East Asia and by more than 4 ppbv over South Asia. In contrast, scenarios that include weak emission controls show increases in surface O_3 of up to 2 ppbv over South Asia.

From the individual source contributions to surface O_3 in 2050, we find most of the benefit for surface O_3 air quality occurs from emission reduction measures in a limited number of sectors, e.g., transport. This highlights where more action to reduce precursor emissions could provide additional benefits to surface O_3, e.g. from agriculture. For regions like Europe and East Asia local emission policies targeting the energy and transport sectors will not be sufficient to achieve substantial O_3 air quality benefits compared to the present day. Benefits can only be achieved by targeting CH_4 sources, as well as local precursor emissions.
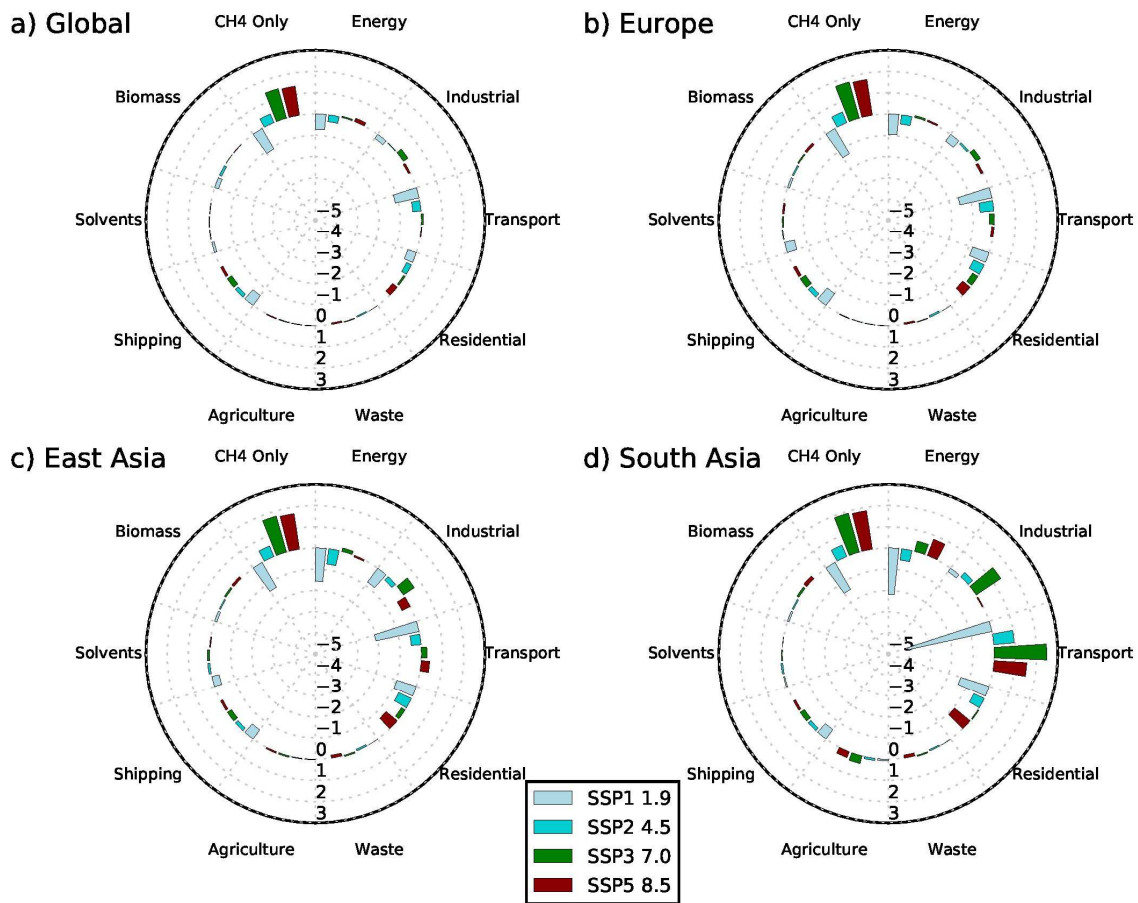
Figure 8 – Changes in annual mean surface O_3 concentrations (ppbv) due to individual emission sectors between 2015 and 2050 for different regions using four different CMIP6 future scenarios.

The contribution of different source sectors to global O_3 radiative forcing in 2050 is shown in Figure 7 and Table S9. The largest source contribution in all scenarios comes from changes in CH_4 abundance, with the energy, waste and agricultural sectors being important sources contributing to changes in CH_4 emissions (Figure S8). For the weak mitigation scenarios (SSP3 7.0 and SSP5 8.5) CH_4 is shown to be the main contributor, causing a positive O_3 radiative forcing in 2050. There are smaller positive contributions under these scenarios from the energy, industrial and transport sectors. For the medium mitigation scenario (SSP2 4.5) the small positive O_3 radiative forcing due to CH_4 is offset by the negative forcing from the energy, transport and residential sectors. For the strongest mitigation scenario (SSP1 1.9) there is a negative O_3 radiative forcing from the energy, transport, residential and shipping sectors, as well as from CH_4, which combine to produce the largest negative O_3 radiative forcing by 2050. Strong reductions in both CH_4 and precursor emissions are needed to reduce the warming effect of O_3. Controlling CH_4 would have the largest impact on reducing future O_3 radiative forcing, as the strong mitigation scenarios show that decreasing CH_4 can significantly reduce the overall positive O_3 radiative forcing, as well as the direct CH_4 radiative forcing.

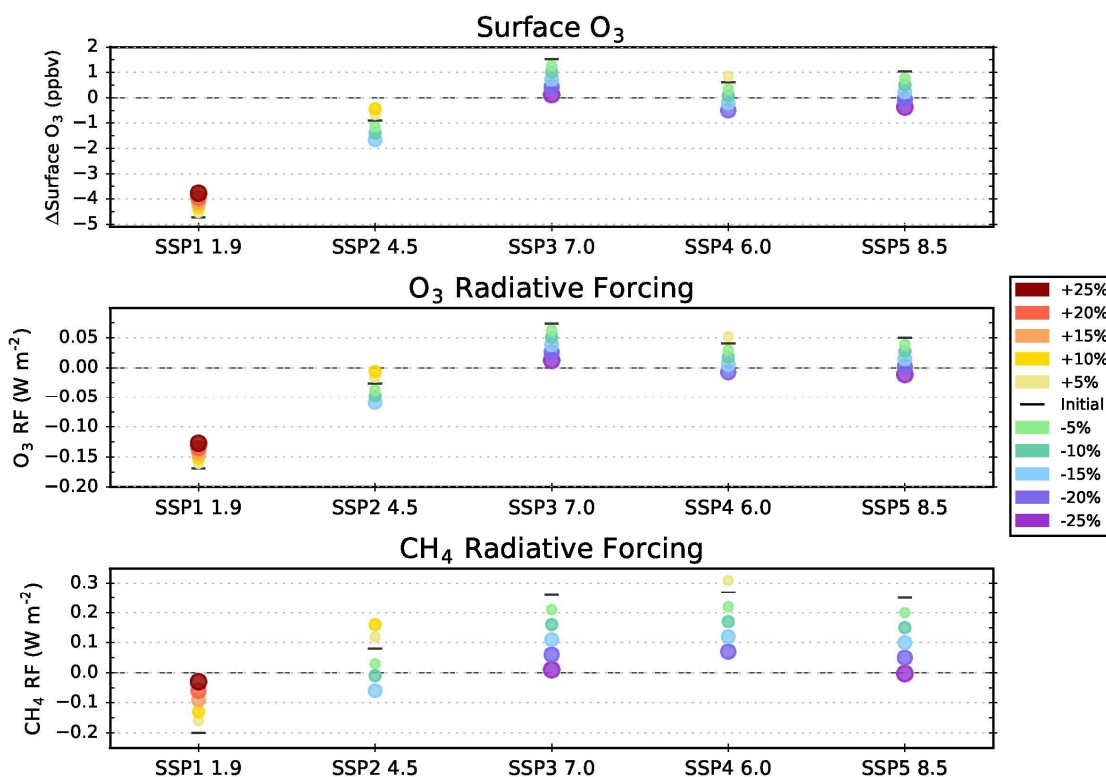### *3.4 Reductions in Global Methane*

To assess the additional benefits from further reductions in global methane we have performed sensitivity experiments with the parameterisation using different values of global CH_4

abundances (-25% to +25%) compared to that in five of the SSPs (Table 4). For all SSPs using lower values of CH_4 (of up to -25%) additionally reduces the predicted global surface O_3 concentration by more than 1 ppbv in 2050 (Table 4 and Figure 9), with larger reductions on a regional scale (Figure S9). For example, the predicted increases in global surface O_3 concentrations in 2050 under the weaker mitigation scenarios (SSP3 7.0, SSP4 6.0 and SSP5 8.5) could be eliminated if the global CH_4 abundance was reduced by 15–25% of the original value used in each scenario. A similar benefit is seen in climate forcing (both O_3 and direct CH_4). The O_3 radiative forcing in SSP1 1.9 would not be as large if the reductions in CH_4 abundances were smaller under this scenario. If larger reductions in global CH_4 abundances occurred for the weaker mitigation scenarios then O_3 radiative forcing in 2050 relative to 2015 could be reduced to near zero, with an additional reduction in the direct CH_4 radiative forcing of up to 0.2 W m^{-2}. Further reductions to the global CH_4 abundance by 2050 would deliver clear additional benefits to surface O_3 air quality and near-term climate forcing (both O_3 and CH_4) under all SSPs.

Table 4 – The response in global surface O_3, O_3 radiative forcing and CH_4 radiative forcing to additional perturbations in CH_4 abundance compared to that in five of the existing SSPs.

Initial SSP Scenario		% change from the initial scenario concentration										
		-25	-20	-15	-10	-5	Initial	+5	+10	+15	+20	+25
SSP1 1.9	ΔCH_4 (ppbv)	-	-	-	-	-	1428	1499	1571	1642	1714	1785
	ΔO_3 (ppbv)	-	-	-	-	-	-4.7	-4.5	-4.3	-4.1	-4.0	-3.8
	O_3 RF (Wm^{-2})	-	-	-	-	-	-0.17	-0.16	-0.15	-0.14	-0.14	-0.13
	CH_4 RF (Wm^{-2})	-	-	-	-	-	-0.20	-0.16	-0.13	-0.09	-0.06	-0.03
SSP2 4.5	ΔCH_4 (ppbv)	-	-	1717	1818	1919	2020	2121	2222	-	-	-
	ΔO_3 (ppbv)	-	-	-1.7	-1.4	-1.2	-0.9	-0.7	-0.4	-	-	-
	O_3 RF (Wm^{-2})	-	-	-0.06	-0.05	-0.04	-0.03	-0.02	-0.01	-	-	-
	CH_4 RF (Wm^{-2})	-	-	-0.06	-0.01	+0.03	+0.08	+0.12	+0.16	-	-	-
SSP3 7.0	ΔCH_4 (ppbv)	1854	1978	2101	2225	2348	2472	-	-	-	-	-
	ΔO_3 (ppbv)	+0.1	+0.4	+0.7	+1.0	+1.3	+1.5	-	-	-	-	-
	O_3 RF (Wm^{-2})	+0.01	+0.03	+0.04	+0.05	+0.06	+0.07	-	-	-	-	-
	CH_4 RF (Wm^{-2})	+0.01	+0.06	+0.11	+0.16	+0.21	+0.26	-	-	-	-	-
SSP4 6.0	ΔCH_4 (ppbv)	-	2003	2128	2253	2378	2504	2629	-	-	-	-
	ΔO_3 (ppbv)	-	-0.5	-0.2	+0.1	+0.4	+0.6	+0.9	-	-	-	-
	O_3 RF (Wm^{-2})	-	-0.01	+0.01	+0.02	+0.03	+0.04	+0.05	-	-	-	-
	CH_4 RF (Wm^{-2})	-	+0.07	+0.12	+0.17	+0.22	+0.27	+0.31	-	-	-	-
SSP5 8.5	ΔCH_4 (ppbv)	1835	1957	2079	2202	2324	2446	-	-	-	-	-
	ΔO_3 (ppbv)	-0.4	-0.1	+0.2	+0.5	+0.8	+1.0	-	-	-	-	-
	O_3 RF (Wm^{-2})	-0.01	+0.00	+0.01	+0.03	+0.04	+0.05	-	-	-	-	-
	CH_4 RF (Wm^{-2})	+0.00	+0.05	+0.10	+0.15	+0.20	+0.25	-	-	-	-	-

Surface O$_3$

O$_3$ Radiative Forcing

CH$_4$ Radiative Forcing

447

Figure 9 – Changes in the global annual mean response of surface O$_3$ concentrations, O$_3$ radiative forcing and direct CH$_4$ radiative forcing in 2050 due to different amounts of methane mitigation assumed in a particular SSP.

4.0 Conclusions

We have used a parameterisation based on source-receptor relationships to predict changes in tropospheric O$_3$ and its radiative forcing over the period 1750 to 2050. Changes in CH$_4$ abundance and O$_3$ precursor emissions (NOx, CO and NMVOCs) from historical and future scenarios of the CMIP6 emission dataset are used within the parameterisation. This allows an initial assessment of the full range of CMIP6 scenarios to be conducted prior to full chemistry climate modelling studies.

Using changes in precursor emissions and CH$_4$ abundances over the industrial period (1750-2014) we find changes in surface O$_3$, tropospheric O$_3$ burden and O$_3$ radiative forcing of +8 ppbv, +76 Tg and +0.3 W m^{-2}. These changes in O$_3$ over the historical period are within the range of multi-model changes simulated in the ACCMIP project, although the parameterisation does not account for changes in climate, stratosphere-to-troposphere exchange or chemical regime (O$_3$ production/titration). There is a much better agreement over the historical period between the parameterisation and ACCMIP if the impact of climate change on tropospheric O$_3$ is accounted for.

Nine future SSPs are used to explore changes to tropospheric O$_3$ over the period 2014 to 2050, when the effects of climate change are assumed to be small. Future scenarios that include strong climate and air pollutant mitigation measures show reductions in global surface O$_3$ concentrations of more than 3.5 ppbv and have a global O$_3$ radiative forcing of less than -0.1 W m^{-2}. There is an additional benefit in these scenarios from the reduction in direct CH$_4$

471 radiative forcing, to less than -0.15 W m^{-2}. Large reductions in surface O_3 occur across the
472 Middle East and South Asia, due to substantial reductions in O_3 precursor emissions and
473 global CH_4 abundance. These reductions will benefit both future surface O_3 air quality and
474 near-term climate forcing but remain well above pre-industrial values.

475 Surface O_3 increases across all regions in future scenarios with assumed weak climate and
476 air pollutant mitigation measures, with the largest increase of >6 ppbv over South Asia. The
477 weak mitigation scenarios result in an O_3 radiative forcing of >+0.05 W m^{-2}, along with a direct
478 CH_4 radiative forcing of up to +0.27 W m^{-2}. This highlights that without reductions to O_3
479 precursor emissions, particularly CH_4, it will not be possible to prevent the future degradation
480 of surface O_3 air quality and the enhancement of anthropogenic climate forcing.

481 A source attribution for East Asia shows that any benefits to surface O_3 from reducing local
482 emission sources could be offset by intercontinental transport of O_3 formed from sources
483 remote to the region and that from global CH_4 sources. In contrast, for South Asia local sources
484 of O_3 are shown to be more important than those remote to the region. Global CH_4 and the
485 transport, industrial and energy sectors have the largest contribution to changes in surface O_3.
486 Our analysis shows that local emission control measures are required alongside
487 intercontinental controls to provide regional benefits to future air quality and near-term climate
488 forcing. In particular, the level of climate mitigation measures for CH_4 within a scenario has a
489 strong influence on the magnitude of benefits that can be achieved. Additional reductions in
490 global CH_4 abundance within a scenario have the potential to provide larger benefits for air
491 quality and climate.

492 The O_3 parameterisation used here provides an easy-to-use tool with which to rapidly assess
493 the impact on tropospheric O_3 from a large range of future emission scenarios. The results of
494 this study highlight the need for emission reduction measures both locally and internationally,
495 particularly for CH_4. While not replacing full model simulations, the tool can provide useful
496 information on a range of future trajectories for tropospheric O_3. This is particularly valuable
497 for modelling centres conducting full chemistry-climate model simulations, allowing them to
498 make better informed decisions on selecting a more limited range of scenarios for detailed
499 analysis.

References

506 Cionni, I., Eyring, V., Lamarque, J.F., Randel, W.J., Stevenson, D.S., Wu, F., Bodeker, G.E., Shepherd, T.G.,
507   Shindell, D.T., Waugh, D.W., 2011. Ozone database in support of CMIP5 simulations: results and
508   corresponding radiative forcing. Atmos. Chem. Phys. Atmos. Chem. Phys. 11, 11267–11292.
509   https://doi.org/10.5194/acp-11-11267-2011

510 Collins, J.W., Lamarque, J.F., Schulz, M., Boucher, O., Eyring, V., Hegglin, I.M., Maycock, A., Myhre, G., Prather,
511   M., Shindell, D., Smith, J.S., 2017. AerChemMIP: Quantifying the effects of chemistry and aerosols in
512   CMIP6. Geosci. Model Dev. 10, 585–607. https://doi.org/10.5194/gmd-10-585-2017

513 Doherty, R.M., Heal, M.R., O'Connor, F.M., 2017. Climate change impacts on human health over Europe through
514   its effect on air quality. Environ. Heal. 16, 118. https://doi.org/10.1186/s12940-017-0325-2

515 Doherty, R.M., Wild, O., Shindell, D.T., Zeng, G., MacKenzie, I.A., Collins, W.J., Fiore, A.M., Stevenson, D.S.,

516   Dentener, F.J., Schultz, M.G., Hess, P., Derwent, R.G., Keating, T.J., 2013. Impacts of climate change on
517   surface ozone and intercontinental ozone pollution: A multi-model study. J. Geophys. Res. Atmos. 118,
518   3744–3763. https://doi.org/10.1002/jgrd.50266

519   Etminan, M., Myhre, G., Highwood, E.J., Shine, K.P., 2016. Radiative forcing of carbon dioxide, methane, and
520   nitrous oxide: A significant revision of the methane radiative forcing. Geophys. Res. Lett. 43, 12,614-
521   12,623. https://doi.org/10.1002/2016GL071930

522   Fiore, A.M., Dentener, F.J., Wild, O., Cuvelier, C., Schultz, M.G., Hess, P., Textor, C., Schulz, M., Doherty, R.M.,
523   Horowitz, L.W., MacKenzie, I.A., Sanderson, M.G., Shindell, D.T., Stevenson, D.S., Szopa, S., Van
524   Dingenen, R., Zeng, G., Atherton, C., Bergmann, D., Bey, I., Carmichael, G., Collins, W.J., Duncan, B.N.,
525   Faluvegi, G., Folberth, G., Gauss, M., Gong, S., Hauglustaine, D., Holloway, T., Isaksen, I.S.A., Jacob,
526   D.J., Jonson, J.E., Kaminski, J.W., Keating, T.J., Lupu, A., Manner, E., Montanaro, V., Park, R.J., Pitari, G.,
527   Pringle, K.J., Pyle, J.A., Schroeder, S., Vivanco, M.G., Wind, P., Wojcik, G., Wu, S., Zuber, A., 2009.
528   Multimodel estimates of intercontinental source-receptor relationships for ozone pollution. J. Geophys. Res.
529   Atmos. 114, 1–21. https://doi.org/10.1029/2008JD010816

530   Fiore, A.M., Naik, V., Leibensperger, E.M., 2015. Air Quality and Climate Connections. J. Air Waste Manage.
531   Assoc. 65, 645–685. https://doi.org/10.1080/10962247.2015.1040526

532   Fiore, A.M., Naik, V., Spracklen, D. V, Steiner, A., Unger, N., Prather, M., Bergmann, D., Cameron-Smith, P.J.,
533   Cionni, I., Collins, W.J., Dalsøren, S., Eyring, V., Folberth, G. a, Ginoux, P., Horowitz, L.W., Josse, B.,
534   Lamarque, J.-F., MacKenzie, I. a, Nagashima, T., O'Connor, F.M., Righi, M., Rumbold, S.T., Shindell, D.T.,
535   Skeie, R.B., Sudo, K., Szopa, S., Takemura, T., Zeng, G., 2012. Global air quality and climate. Chem. Soc.
536   Rev. 41, 6663–83. https://doi.org/10.1039/c2cs35095e

537   Fowler, D., Pilegaard, K., Sutton, M.A., Ambus, P., Raivonen, M., Duyzer, J., Simpson, D., Fagerli, H., Fuzzi, S.,
538   Schjoerring, J.K., Granier, C., Neftel, A., Isaksen, I.S.A., Laj, P., Maione, M., Monks, P.S., Burkhardt, J.,
539   Daemmgen, U., Neirynck, J., Personne, E., Wichink-Kruit, R., Butterbach-Bahl, K., Flechard, C., Tuovinen,
540   J.P., Coyle, M., Gerosa, G., Loubet, B., Altimir, N., Gruenhage, L., Ammann, C., Cieslik, S., Paoletti, E.,
541   Mikkelsen, T.N., Ro-Poulsen, H., Cellier, P., Cape, J.N., Horváth, L., Loreto, F., Niinemets, Ü., Palmer, P.I.,
542   Rinne, J., Misztal, P., Nemitz, E., Nilsson, D., Pryor, S., Gallagher, M.W., Vesala, T., Skiba, U.,
543   Brüggemann, N., Zechmeister-Boltenstern, S., Williams, J., O'Dowd, C., Facchini, M.C., de Leeuw, G.,
544   Flossman, A., Chaumerliac, N., Erisman, J.W., 2009. Atmospheric composition change: Ecosystems–
545   Atmosphere interactions. Atmos. Environ. 43, 5193–5267. https://doi.org/10.1016/j.atmosenv.2009.07.068

546   Gaudel, A., Cooper, O.R., Ancellet, G., Barret, B., Boynard, A., Burrows, J.P., Clerbaux, C., Coheur, P.-F.,
547   Cuesta, J., Cuevas, E., Doniki, S., Dufour, G., Ebojie, F., Foret, G., Garcia, O., Granados-Muñoz, M.J.,
548   Hannigan, J.W., Hase, F., Hassler, B., Huang, G., Hurtmans, D., Jaffe, D., Jones, N., Kalabokas, P.,
549   Kerridge, B., Kulawik, S., Latter, B., Leblanc, T., Le Flochmoën, E., Lin, W., Liu, J., Liu, X., Mahieu, E.,
550   McClure-Begley, A., Neu, J.L., Osman, M., Palm, M., Petetin, H., Petropavlovskikh, I., Querel, R., Rahpoe,
551   N., Rozanov, A., Schultz, M.G., Schwab, J., Siddans, R., Smale, D., Steinbacher, M., Tanimoto, H.,
552   Tarasick, D.W., Thouret, V., Thompson, A.M., Trickl, T., Weatherhead, E., Wespes, C., Worden, H.M.,
553   Vigouroux, C., Xu, X., Zeng, G., Ziemke, J., Helmig, D., Lewis, A., 2018. Tropospheric Ozone Assessment
554   Report: Present-day distribution and trends of tropospheric ozone relevant to climate and global
555   atmospheric chemistry model evaluation. Elem Sci Anth 6. https://doi.org/10.1525/elementa.291

556   Gidden, M.J., Riahi, K., Smith, S.J., Fujimori, S., Luderer, G., Kriegler, E., van Vuuren, D.P., van den Berg, M.,
557   Feng, L., Klein, D., Calvin, K., Doelman, J.C., Frank, S., Fricko, O., Harmsen, M., Hasegawa, T., Havlik, P.,
558   Hilaire, J., Hoesly, R., Horing, J., Popp, A., Stehfest, E., Takahashi, K., 2019. Global emissions pathways
559   under different socioeconomic scenarios for use in CMIP6: a dataset of harmonized emissions trajectories
560   through the end of the century. Geosci. Model Dev. 12, 1443–1475. https://doi.org/10.5194/gmd-12-1443-
561   2019

562   Hoesly, R.M., Smith, S.J., Feng, L., Klimont, Z., Janssens-Maenhout, G., Pitkanen, T., Seibert, J.J., Vu, L.,
563   Andres, R.J., Bolt, R.M., Bond, T.C., Dawidowski, L., Kholod, N., Kurokawa, J., Li, M., Liu, L., Lu, Z.,
564   Moura, M.C.P., O&apos;Rourke, P.R., Zhang, Q., 2018. Historical (1750–2014) anthropogenic
565   emissions of reactive gases and aerosols from the Community Emissions Data System (CEDS). Geosci.
566   Model Dev. 11, 369–408. https://doi.org/10.5194/gmd-11-369-2018

567   Iglesias-Suarez, F., Kinnison, D.E., Rap, A., Maycock, A.C., Wild, O., Young, P.J., 2018. Key drivers of ozone
568   change and its radiative forcing over the 21st century. Atmos. Chem. Phys. 18, 6121–6139.
569   https://doi.org/10.5194/acp-18-6121-2018

570   Jacob, D.J., Winner, D. a., 2009. Effect of climate change on air quality. Atmos. Environ. 43, 51–63.
571   https://doi.org/10.1016/j.atmosenv.2008.09.051

572   Jerrett, M., Burnett, R.T., Pope, C.A., Ito, K., Thurston, G., Krewski, D., Shi, Y., Calle, E., Thun, M., 2009. Long-
573   Term Ozone Exposure and Mortality. N. Engl. J. Med. 360, 1085–1095.

574   https://doi.org/10.1056/NEJMoa0803894

575   Kawase, H., Nagashima, T., Sudo, K., Nozawa, T., 2011. Future changes in tropospheric ozone under
576   Representative Concentration Pathways (RCPs). Geophys. Res. Lett. 38, L05801.
577   https://doi.org/10.1029/2010GL046402

578   Kim, M.J., Park, R.J., Ho, C.-H., Woo, J.-H., Choi, K.-C., Song, C.-K., Lee, J.-B., 2015. Future ozone and
579   oxidants change under the RCP scenarios. Atmos. Environ. 101, 103–115.
580   https://doi.org/10.1016/J.ATMOSENV.2014.11.016

581   Lamarque, J.-F., Shindell, D.T., Josse, B., Young, P.J., Cionni, I., Eyring, V., Bergmann, D., Cameron-Smith, P.,
582   Collins, W.J., Doherty, R., Dalsoren, S., Faluvegi, G., Folberth, G., Ghan, S.J., Horowitz, L.W., Lee, Y.H.,
583   MacKenzie, I.A., Nagashima, T., Naik, V., Plummer, D., Righi, M., Rumbold, S.T., Schulz, M., Skeie, R.B.,
584   Stevenson, D.S., Strode, S., Sudo, K., Szopa, S., Voulgarakis, A., Zeng, G., 2013. The Atmospheric
585   Chemistry and Climate Model Intercomparison Project (ACCMIP): overview and description of models,
586   simulations and climate diagnostics. Geosci. Model Dev. 6, 179–206. https://doi.org/10.5194/gmd-6-179-
587   2013

588   Malley, C.S., Henze, D.K., Kuylenstierna, J.C.I., Vallack, H.W., Davila, Y., Anenberg, S.C., Turner, M.C.,
589   Ashmore, M.R., 2017. Updated Global Estimates of Respiratory Mortality in Adults ≥30 Years of Age
590   Attributable to Long-Term Ozone Exposure. Environ. Health Perspect. 125, 87021.
591   https://doi.org/10.1289/EHP1390

592   Myhre, G., Shindell, D., Breon, F.-M., Collins, W., Fuglestvedt, J., Huang, J., Koch, D., Lamarque, J.-F., Lee, D.,
593   Mendoza, B., Nakajima, T., Robock, A., Stephens, G., Takemura, T., Zhang, H., 2013. Anthropogenic and
594   Natural Radiative Forcing. In: Climate Change 2013: The Physical Science Basis. Contribution of Working
595   Group I to the Fifth Assessment Report of the Intergovernemental Panel on Cliamte Change. Cambridge
596   University Press, Cambridge, United Kingdom and New York, NY, USA.

597   O'Connor, F.M., Johnson, C.E., Morgenstern, O., Abraham, N.L., Braesicke, P., Dalvi, M., Folberth, G.A.,
598   Sanderson, M.G., Telford, P.J., Voulgarakis, A., Young, P.J., Zeng, G., Collins, W.J., Pyle, J.A., 2014.
599   Evaluation of the new UKCA climate-composition model – Part 2: The Troposphere. Geosci. Model Dev. 7,
600   41–91. https://doi.org/10.5194/gmd-7-41-2014

601   O'Neill, B.C., Kriegler, E., Riahi, K., Ebi, K.L., Hallegatte, S., Carter, T.R., Mathur, R., van Vuuren, D.P., 2014. A
602   new scenario framework for climate change research: the concept of shared socioeconomic pathways.
603   Clim. Change 122, 387–400. https://doi.org/10.1007/s10584-013-0905-2

604   Rao, S., Klimont, Z., Smith, S.J., Dingenen, R. Van, Dentener, F., Bouwman, L., Riahi, K., Amann, M., Bodirsky,
605   B.L., Van Vuuren, D.P., Reis, L.A., Calvin, K., Drouet, L., Fricko, O., Fujimori, S., Gernaat, D., Havlik, P.,
606   Harmsen, M., Hasegawa, T., Heyes, C., Hilaire, J., Luderer, G., Masui, T., Stehfest, E., Strefler, J., Van Der
607   Sluis, S., Tavoni, M., 2017. Future air pollution in the Shared Socio-economic Pathways. Glob. Environ.
608   Chang. 42, 346–358. https://doi.org/10.1016/j.gloenvcha.2016.05.012

609   Riahi, K., Van Vuuren, D.P., Kriegler, E., Edmonds, J., O 'neill, B.C., Fujimori, S., Bauer, N., Calvin, K., Dellink,
610   R., Fricko, O., Lutz, W., Popp, A., Cuaresma, J.C., Kc, S., Leimbach, M., Jiang, L., Kram, T., Rao, S.,
611   Emmerling, J., Ebi, K., Hasegawa, T., Havlik, P., Humpenöder, F., Aleluia, L., Silva, D., Smith, S., Stehfest,
612   E., Bosetti, V., Eom, J., Gernaat, D., Masui, T., Rogelj, J., Strefler, J., Drouet, L., Krey, V., Luderer, G.,
613   Harmsen, M., Takahashi, K., Baumstark, L., Doelman, J.C., Kainuma, M., Klimont, Z., Marangoni, G.,
614   Lotze-Campen, H., Obersteiner, M., Tabeau, A., Tavoni, M., 2017. The Shared Socioeconomic Pathways
615   and their energy, land use, and greenhouse gas emissions implications: An overview. Glob. Environ.
616   Chang. 42, 153–168. https://doi.org/10.1016/j.gloenvcha.2016.05.009

617   Sellar, A., 2019. UKESM1: description and evaluation of the UK Earth system model. in prep.

618   Stevenson, D.S., Young, P.J., Naik, V., Lamarque, J.-F., Shindell, D.T., Voulgarakis, A., Skeie, R.B., Dalsoren,
619   S.B., Myhre, G., Berntsen, T.K., Folberth, G.A., Rumbold, S.T., Collins, W.J., MacKenzie, I.A., Doherty,
620   R.M., Zeng, G., van Noije, T.P.C., Strunk, A., Bergmann, D., Cameron-Smith, P., Plummer, D.A., Strode,
621   S.A., Horowitz, L., Lee, Y.H., Szopa, S., Sudo, K., Nagashima, T., Josse, B., Cionni, I., Righi, M., Eyring,
622   V., Conley, A., Bowman, K.W., Wild, O., Archibald, A., 2013. Tropospheric ozone changes, radiative forcing
623   and attribution to emissions in the Atmospheric Chemistry and Climate Model Intercomparison Project
624   (ACCMIP). Atmos. Chem. Phys. 13, 3063–3085. https://doi.org/10.5194/acp-13-3063-2013

625   Turner, M.C., Jerrett, M., Pope, C.A., Krewski, D., Gapstur, S.M., Diver, W.R., Beckerman, B.S., Marshall, J.D.,
626   Su, J., Crouse, D.L., Burnett, R.T., 2016. Long-Term Ozone Exposure and Mortality in a Large Prospective
627   Study. Am. J. Respir. Crit. Care Med. 193, 1134–1142. https://doi.org/10.1164/rccm.201508-1633OC

628   Turnock, S.T., Wild, O., Dentener, F.J., Davila, Y., Emmons, L.K., Flemming, J., Folberth, G.A., Henze, D.K.,
629   Jonson, J.E., Keating, T.J., Kengo, S., Lin, M., Lund, M., Tilmes, S., O'Connor, F.M., 2018. The impact of
630   future emission policies on tropospheric ozone using a parameterised approach. Atmos. Chem. Phys. 18,

631   8953–8978. https://doi.org/10.5194/acp-18-8953-2018

632 United Nations, 2016. Paris Agreement.

633 van Vuuren, D.P., Kriegler, E., O'Neill, B.C., Ebi, K.L., Riahi, K., Carter, T.R., Edmonds, J., Hallegatte, S., Kram,
634   T., Mathur, R., Winkler, H., 2014. A new scenario framework for Climate Change Research: scenario matrix
635   architecture. Clim. Change 122, 373–386. https://doi.org/10.1007/s10584-013-0906-1

636 von Schneidemesser, E., Monks, P.S., Allan, J.D., Bruhwiler, L., Forster, P., Fowler, D., Lauer, A., Morgan, W.T.,
637   Paasonen, P., Righi, M., Sindelarova, K., Sutton, M. a., 2015. Chemistry and the Linkages between Air
638   Quality and Climate Change. Chem. Rev. 115, 3856–3897. https://doi.org/10.1021/acs.chemrev.5b00089

639 Wild, O., Fiore, A.M., Shindell, D.T., Doherty, R.M., Collins, W.J., Dentener, F.J., Schultz, M.G., Gong, S.,
640   Mackenzie, I.A., Zeng, G., Hess, P., Duncan, B.N., Bergmann, D.J., Szopa, S., Jonson, J.E., Keating, T.J.,
641   Zuber, A., 2012. Modelling future changes in surface ozone: A parameterized approach. Atmos. Chem.
642   Phys. 12, 2037–2054. https://doi.org/10.5194/acp-12-2037-2012

643 Young, P.J., Archibald, A.T., Bowman, K.W., Lamarque, J.-F., Naik, V., Stevenson, D.S., Tilmes, S., Voulgarakis,
644   A., Wild, O., Bergmann, D., Cameron-Smith, P., Cionni, I., Collins, W.J., Dalsøren, S.B., Doherty, R.M.,
645   Eyring, V., Faluvegi, G., Horowitz, L.W., Josse, B., Lee, Y.H., MacKenzie, I.A., Nagashima, T., Plummer,
646   D.A., Righi, M., Rumbold, S.T., Skeie, R.B., Shindell, D.T., Strode, S.A., Sudo, K., Szopa, S., Zeng, G.,
647   2013. Pre-industrial to end 21st century projections of tropospheric ozone from the Atmospheric Chemistry
648   and Climate Model Intercomparison Project (ACCMIP). Atmos. Chem. Phys. 13, 2063–2090.
649   https://doi.org/10.5194/acp-13-2063-2013

650 Young, P.J., Naik, V., Fiore, A.M., Gaudel, A., Guo, J., Lin, M.Y., Neu, J.L., Parrish, D.D., Rieder, H.E., Schnell,
651   J.L., Tilmes, S., Wild, O., Zhang, L., Ziemke, J.R., Brandt, J., Delcloo, A., Doherty, R.M., Geels, C.,
652   Hegglin, M.I., Hu, L., Im, U., Kumar, R., Luhar, A., Murray, L., Plummer, D., Rodriguez, J., Saiz-Lopez, A.,
653   Schultz, M.G., Woodhouse, M.T., Zeng, G., 2018. Tropospheric Ozone Assessment Report: Assessment of
654   global-scale model performance for global and regional ozone distributions, variability, and trends. Elem
655   Sci Anth 6, 10. https://doi.org/10.1525/elementa.265

656